Journal of Reinforced Plastics and Composites

published on September 4, 2008

http://dx.doi.org/10.1177/0731684408092453

Analysis of Dry Sliding Wear Behavior of Red Mud Filled Polyester Composites using the Taguchi Method

ALOK SATAPATHY*
Department of Mechanical Engineering National Institute of Technology Rourkela 769008, India

AMAR PATNAIK
Department of Mechanical Engineering National Institute of Technology, Hamirpur-177005, India

E-mal: satapathy.alok@gmail.com

Analysis of Dry Sliding Wear Behavior of Red Mud Filled Polyester Composites using the Taguchi Method

ALOK SATAPATHY*
Department of Mechanical Engineering National Institute of Technology Rourkela 769008, India

AMAR PATNAIK
Department of Mechanical Engineering National Institute of Technology, Hamirpur-177005, India

ABSTRACT: Red mud is an industrial waste generated during the production of alumina by Bayer's process. Using this red mud as the filler, particulate reinforced polyester composites have been prepared and their dry sliding wear behavior has been studied experimentally. For this a standard pin-on-disc test set-up and Taguchi's orthogonal arrays were used. Taguchi's experimental design method eliminates the need for repeated experiments and thus saves time, materials, and cost. It identifies the significant control factors and their interactions predominantly influencing the wear rate. From the experimental findings, an optimal combination of control factors was obtained on the basis of which a predictive model was proposed. This model was validated by performing a confirmation experiment with an arbitrarily chosen set of factor combinations. Finally, the optimal factor settings for minimum wear rate under specified experimental conditions have been determined using a genetic algorithm.

KEY WORDS: sliding wear, polyester, red mud, Taguchi method, genetic algorithm.

INTRODUCTION

POLYMERS HAVE GENERATED wide interest in various engineering fields including tribological applications, in view of their good strength and low density as compared to monolithic metal alloys. Being lightweight they are the most suitable materials for weight sensitive uses, but their high cost sometimes becomes the limiting factor for commercial applications. Use of low cost, easily available fillers is therefore useful to bring down the cost of components. Study of the effect of such filler addition is necessary to ensure that the mechanical properties of the composites are not affected adversely by such addition. Available references suggest a large number of materials to be used as fillers in polymers [1]. The purpose of use of fillers can therefore be divided into two basic categories; first, to improve the mechanical, thermal or tribological properties, and second, to reduce the cost of the component. There have been various reports on the use of materials such as minerals and inorganic oxides (alumina and silica), mixed into widely used thermoplastic polymers like polypropylene

*Author to whom correspondence should be addressed. E-mal: satapathy.alok@gmail.com

[2,3] and polyethylene [4,5]. But very few attempts have indeed been made to utilize cheap materials like industrial wastes in preparing particle-reinforced polymer composites.

A key feature of particulate-reinforced polymer composites that makes them so promising as engineering materials is the opportunity to tailor the properties of the materials through the control of filler content and matrix combinations and the selection of processing techniques. A judicious selection of matrix and the reinforcing solid particulate phase can lead to a composite with a combination of strength and modulus comparable to or even better than those of conventional metallic materials [6]. Hard particulate fillers consisting of ceramic or metal particles and fiber fillers made of glass are being used these days to dramatically improve the wear resistance of composites, even up to three orders of magnitude [7]. The improved performance of polymers and their composites in industrial and structural applications by the addition of particulate fillers has shown great promise and so has lately been the subject of considerable interest. Various kinds of polymers and polymer–matrix composites reinforced with metal particles have a wide range of industrial applications such as heaters, electrodes [8], composites with thermal durability at high temperature [9], etc. These engineering composites are desired due to their low density, high corrosion resistance, ease of fabrication, and low cost [10,11]. Similarly, ceramic filled polymer composites have been the subject of extensive research in the past twenty years.

Red mud, as the name suggests, is brick red in color and slimy with an average particle size of about 80 μm. It is comprised of the iron, titanium, and the silica part of the parent ore along with other minor constituents. It is alkaline, thixotropic, and possesses high surface area in the range of 13–16 m^2/g with a true density of 3.30 g/cm^3. The leaching chemistry of bauxite suggests that the physical and chemical properties of red mud depend on the bauxite used and the manner in which the bauxite is processed. Residues from different bauxite have a wide range of composition: Fe_2O_3 20–60%, Al_2O_3 10–30%, SiO_2 2–20%, Na_2O 2–10%, CaO 2–8%, TiO_2 traces 2–8%. Detailed characterization of red mud generated from NALCO aluminum refinery at Damanjodi, India is reported by Mohapatra et al. [12] and of some other sources by various authors [13–15]. This low-cost filler has been used in some earlier studies with different polymer matrices such as polypropylene [16] and nylon [17] to study the mechanical properties in tension and compression. The role of ceramic particles in the wear behavior of composites has also been studied by some researchers. A number of experiments have been performed using different ceramics such as Al_2O_3, TiC, and SiC by varying the particle size and particle volume fraction [18].

To study the correlation between the wear properties and the characteristic parameters, e.g., the composition of the composite and the operating conditions, is of prime importance for designing proper composites in order to satisfy various functional requirements. But visualization of impact of any individual control factor in an interacting environment really becomes difficult. To this end, an attempt has been made in this study to analyze the impact of more than one parameter on sliding wear of the polyester red mud composite. It is important as in actual practice the resultant wear rate is the combined effect of more than one interacting variable. An inexpensive and easy-to-operate experimental strategy based on Taguchi's parameter design has been adopted to study the effect of various parameters and their interactions. This experimental procedure has been successfully applied for parametric appraisal in the wire electrical discharge machining (WEDM) process, drilling of metal matrix composites, and erosion behavior of polymer–matrix composites [19–21]. Finally, the optimal factor settings for minimum wear rate have been determined using a popular evolutionary approach known as the genetic algorithm because it has the capability of finding out global optimum in a large search space.

EXPERIMENTAL DETAILS

Specimen Preparation

Red mud collected from NALCO aluminum refinery at Damanjodi, India is sieved to obtain a particle size in the range 70–90 μm. These particles are reinforced in unsaturated isophthalic polyester resin (modulus 3.25 GPa, density 1.35 gm/cm^3) to prepare the composites. Two percent (2%) cobalt nephthalate (as accelerator) is mixed thoroughly in isophthalic polyester resin followed by 2% methyl-ethyl-ketone-peroxide (MEKP) as hardener resin prior to reinforcement. The dough (polyester resin mixed with red mud) is then slowly decanted into the glass tubes, coated beforehand with uniform thin film of silicone-releasing agent. The composites are cast by conventional hand-lay-up technique in glass tubes so as to get cylindrical specimens (Φ9 mm, length 120 mm). Composites of three different compositions (10, 20, and 30 wt% red mud filling) are made. The castings are left to cure at room temperature for about 24 h after which the tubes are broken and samples are released. Specimens of suitable dimension are cut using a diamond cutter for further physical characterization and wear test.

Test of Microhardness, Tensile Strength, and Density

Microhardness measurement is done using a Leitz microhardness tester. A diamond indentor, in the form of a right pyramid with a square base and an angle of 136° between opposite faces, is forced into the material under a load P. The two diagonals X and Y of the indentation left in the surface of the material after removal of the load are measured and their arithmetic mean d is calculated. In the present study, the load 'L' equals 24.54 N and Vickers hardness number is calculated as:

$$H_V = 0.1889\frac{L}{d^2} \tag{1}$$

and $d = (X + Y)/2$, where d is the diagonal of square impression (mm), X is the horizontal length (mm) and Y is the vertical length (mm).

The tensile test is generally performed on flat specimens. The commonly used specimens used for the tensile test are the dog-bone specimen and straight side specimen with end tabs. A uniaxial load is applied through both ends. The ASTM standard test method for tensile properties of particulate filled polymer composites has the designation D 638 M91. The length of the test section should be 180 mm. The tensile test is performed in the universal testing machine Instron 1195 and results are analyzed to calculate the tensile strength of composite samples.

The worn surfaces of the specimens are examined directly by scanning electron microscope JEOL JSM-6480LV. The worn samples are mounted on stubs with silver paste. To enhance the conductivity of the samples, a thin film of platinum is vacuum-evaporated onto them before the photomicrographs are taken.

Sliding Wear Test

To evaluate the performance of these composites under dry sliding condition, wear tests are carried out in a pin-on-disc type friction and wear monitoring test rig

Table 1. Levels of the variables used in the experiment.

	Level			
Control factor	**I**	**II**	**III**	**Units**
A: Sliding velocity	100	200	300	cm/s
B: Red mud content	10	20	30	wt%
C: Normal load	10	15	20	N

(supplied by DUCOM) as per ASTM G 99. The counter body is a disc made of hardened ground steel (EN-32, hardness 72 HRC, surface roughness 0.6 μ Ra). The specimen is held stationary and the disc is rotated while a normal force is applied through a lever mechanism. A series of tests are conducted with three sliding velocities of 100, 200, and 300 cm/s under three different normal loadings of 10, 15, and 20 N. The material loss from the composite surface is measured using a precision electronic balance with accuracy ±0.1 mg and the specific wear rate (mm^3/N-m) is then expressed on 'volume loss' basis as:

$$W_s = \frac{\Delta m}{\rho t} V_s \cdot F_n \tag{2}$$

where Δm is the mass loss in the test duration (g), ρ is the density of the composite (g/mm^3), t is the test duration (s), V_s is the sliding velocity (m/s), and F_n is the average normal load (N).

The specific wear rate is defined as the volume loss of the specimen per unit sliding distance per unit applied normal load.

Experimental Design

Design of experiment is a powerful analysis tool for modeling and analyzing the influence of control factors on performance output. The most important stage in the design of experiment lies in the selection of the control factors. Therefore, a number of factors are included so that non-significant variables can be identified at the earliest opportunity. The wear tests are carried out under operating conditions given in Table 1.

Three parameters, viz., sliding velocity, redmud content, and normal load each at three levels, are considered in this study in accordance with L_{27} (3^{13}) orthogonal array design. The S/N ratio for minimum wear rate coming under 'smaller is the better characteristic', can be calculated as the logarithmic transformation of the loss function as shown below.

Smaller is the better characteristic:

$$\frac{S}{N} = -10 \log \frac{1}{n} \left(\sum y^2 \right) \tag{3}$$

where n is the number of observations, and y is the observed data. 'Lower is better' (LB) characteristic, with the above S/N ratio transformation, is suitable for minimization of wear rate. The standard linear graph, as shown in Figure 1, is used to assign the factors and interactions to various columns of the orthogonal array [22].

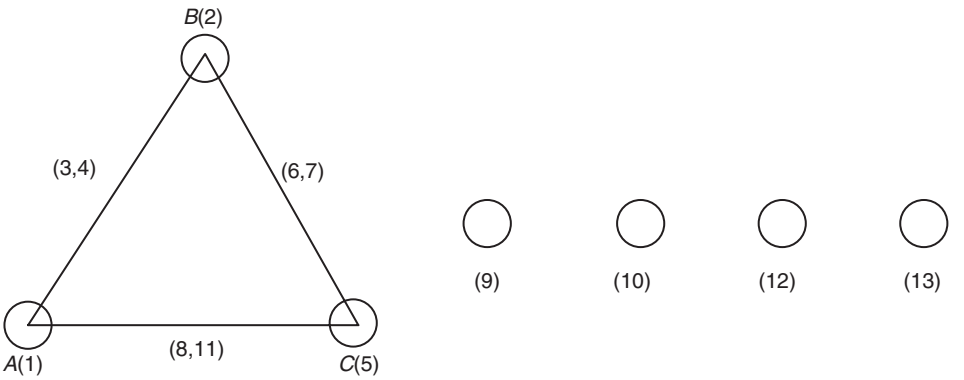

Figure 1. *Standard linear graphs for L_{27} array.*

RESULTS AND DISCUSSION

Density, Micro-hardness, and Tensile Strength

With inclusion of red mud particles in the polymer matrix the density of the composite is found to be increasing. The densities of the three different samples (with 10, 20, and 30 wt% of red mud) are measured as 1.67, 1.81, and 1.93 g/cm^3 respectively. The improvement in density is obvious as the true density of red mud is about 2.5 times that of neat polyester. The micro-hardness values recorded in Vickers' scale for the composites are 54, 59, and 62 Hv respectively. It is found to be increasing with the red mud content in the composites.

The test results for tensile strengths are shown in Figure 2. It is seen that in all the samples the tensile strength of the composites decrease with increase in filler content. The neat polyester has a strength of 174 MPa in tension and it is seen from figure *x* that this value drops to 162.3 MPa with the inclusion of 10 wt% of red mud. The tensile strength of the composite further drops to 156.7 and 151.3 MPa in the case of the other two composites with 20 and 30 wt% of red mud, respectively. There can be two reasons for this decline in strength; one possibility is that the chemical reaction at the interface between the filler particles and the matrix may be too weak to transfer the tensile stress; the other is that the corner points of the irregular-shaped particulates result in stress concentration in the polyester matrix. These two factors are responsible for reducing the tensile strengths of the composites so significantly.

Dry Sliding Wear Analysis

The scanning electron micrograph of raw red mud powder is shown in Figure 3. It is seen that while most of the particles are nearly spherical in shape, many of them are also irregular shaped having sharp edges. The morphology of the worn surface of polyester composite with 10 wt% red mud is illustrated in Figure 4. This micrograph is taken after 3 h of test duration with a sliding velocity of 200 cm/s under a normal load of 20 N. It can be seen that there is a plastic flow of the matrix material in the sliding direction which is indicated by the arrow. It is understandable that with increase in applied load and/or sliding velocity, the thermoplastic polyester softens due to frictional heat generation. As a

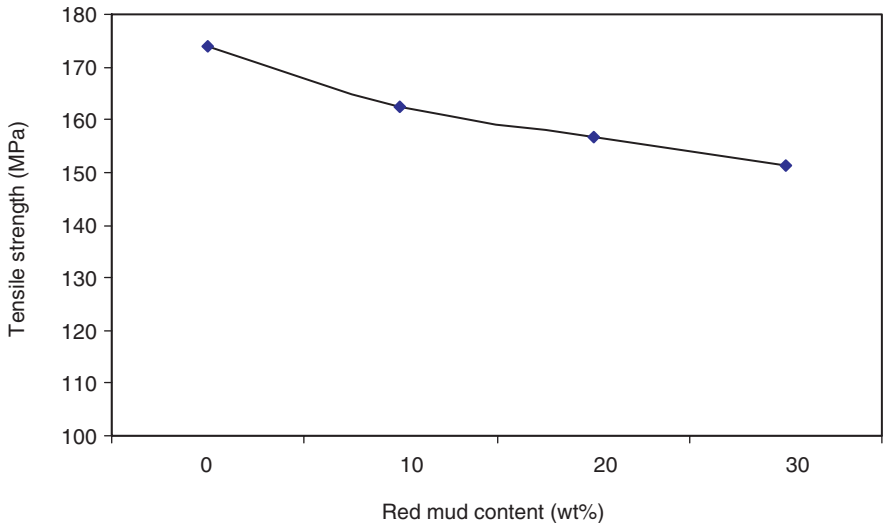

Figure 2. *Variation of tensile strength with red mud content.*

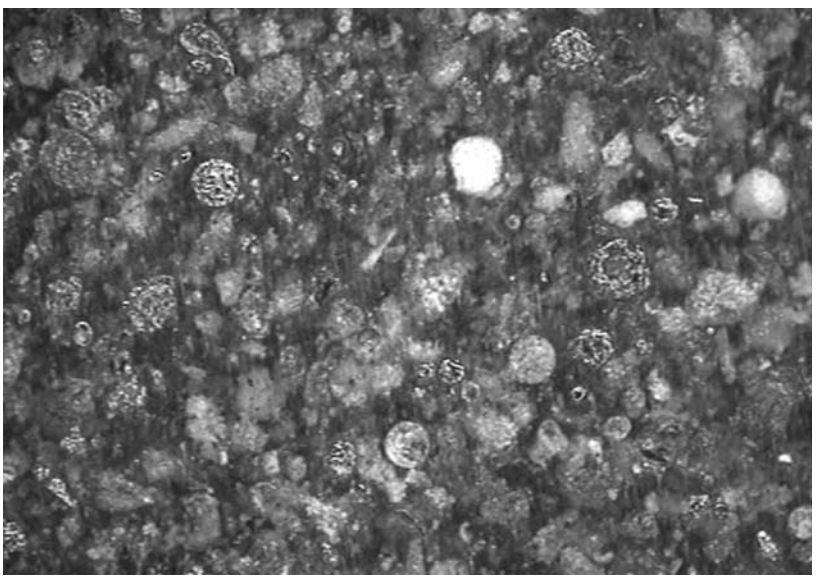

Figure 3. *SEM micrograph of the red mud particles.*

result, the red mud particles, which are brittle in nature and have sharp edges, easily tear the matrix and gradually get aligned along the sliding direction. These particles by virtue of their size, shape, brittleness, and high harness influence modify the wear behavior of the composites. In the process, the red mud particles are dispersed and coagulated in a different manner. Longer duration of sliding results in formation of wear debris of different sizes and shapes. A typical micrograph of small and medium sized wear debris collected during the test after a sliding distance of about 3000 m is shown in Figure 5. The specific wear rates obtained for all the 27 test runs are presented in Figure 6.

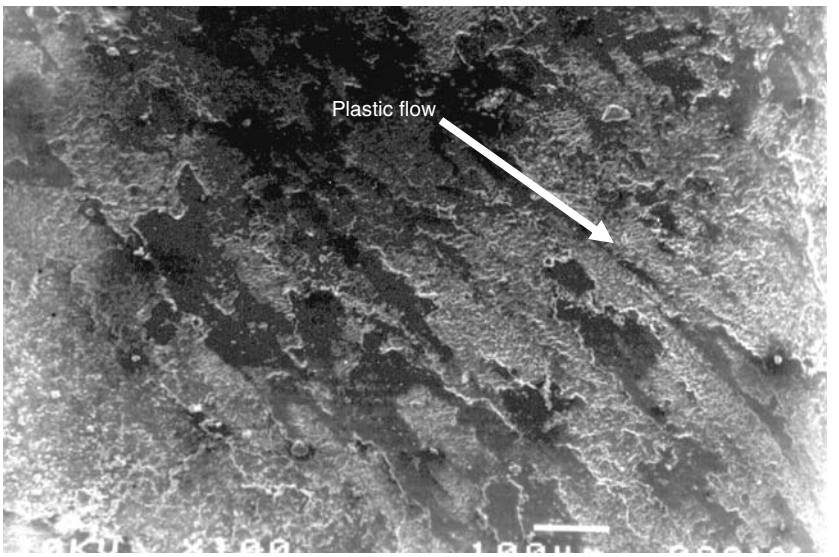

Figure 4. *SEM micrograph of worn composite surface ($V_s = 200$ cm/s, $F_n = 20$ N).*

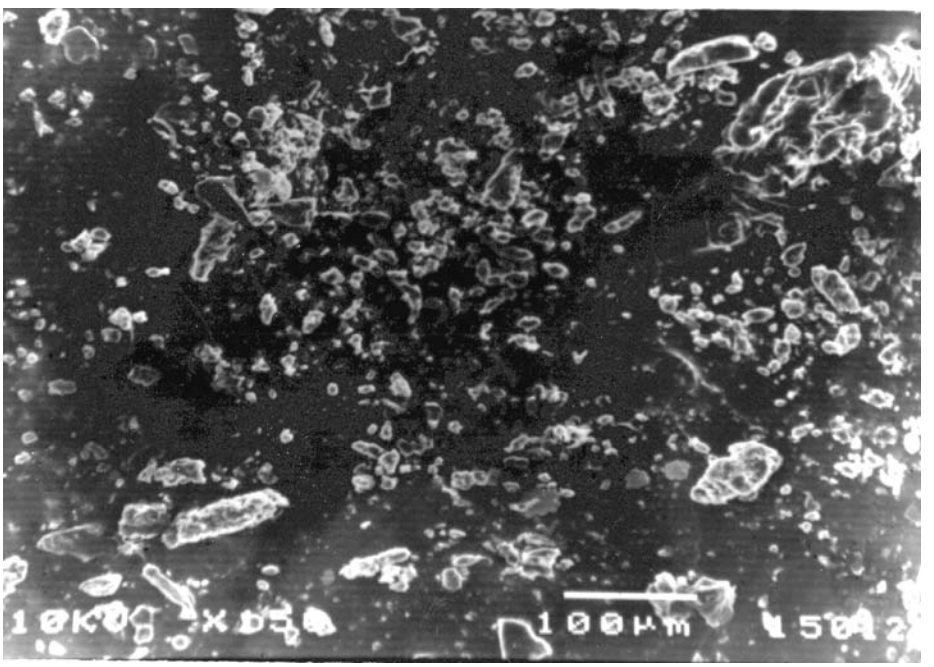

Figure 5. *SEM micrograph of wear debris.*

From Table 2, the overall mean for the S/N ratio of the wear rate is found to be –7.50 dB. Figure 7 shows graphically the effect of the three control factors on specific wear rate. The analyses are made using the popular software specifically used for design of experiment applications known as MINITAB 14. Before any attempt is made to use this

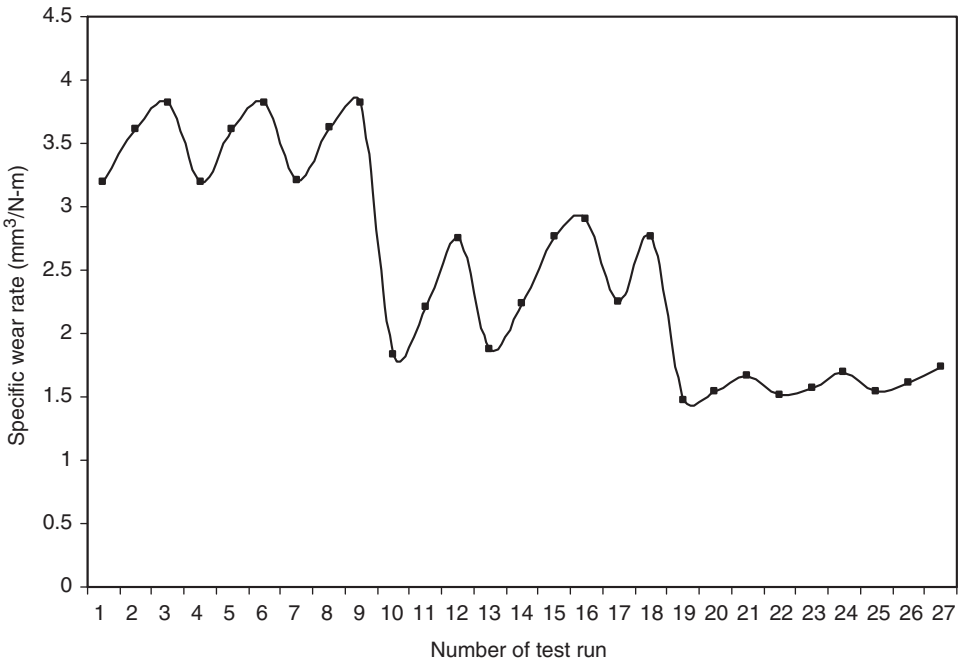

Figure 6. *Specific wear rates under different test conditions.*

simple model as a predictor for the measures of performance, the possible interactions between the control factors must be considered. Thus factorial design incorporates a simple means of testing for the presence of the interaction effects.

Analysis of the results leads to the conclusion that factor combination of A_3, B_1, and C_1 gives minimum specific wear rate. The interaction graphs are shown in Figures 8, 9 and 10. As far as minimization of specific wear rate is concerned, factor A and C have significant effect whereas factor B has least effect. It is observed from Figure 8 that the interaction between $A \times B$ shows least significant effect on specific wear rate. Although the factor B individually has relatively less contribution on output performance, but its interaction with factor C has significant contribution on minimization of specific wear rate (Figure 9). On the other hand, the factors A, C and their interaction ($A \times C$) have major contribution on specific wear rate (Figure 10).

ANOVA and the Effects of Factors

In order to understand a concrete visualization of impact of various factors and their interactions, it is desirable to develop an analysis of variance (ANOVA) table to find out the order of significant factors as well as interactions. Table 3 shows the results of the ANOVA with the specific wear rate. This analysis is undertaken for a level of confidence of significance of 5%. The last column of the table indicates the order of significance among factors and interactions.

From Table 3, we can observe that the sliding velocity ($p = 0.000$) and normal load ($p = 0.004$) have great influence on specific wear rate. The interaction of sliding velocity $\times$ normal load ($p = 0.203$) and red mud content $\times$ normal load ($p = 0.447$)

Table 2. Experimental design using L_{27} orthogonal array.

L_{27} (3^{13})	Sliding velocity (cm/s)	Red mud content (wt%)	Normal load (N)	Specific wear rate (mm^3/N-m)	S/N ratio (dB)
1	100	10	10	3.18774	−10.0697
2	100	10	15	3.61269	−11.1566
3	100	10	20	3.81787	−11.6364
4	100	20	10	3.19730	−10.0957
5	100	20	15	3.61719	−11.1674
6	100	20	20	3.82067	−11.6428
7	100	30	10	3.20649	−10.1206
8	100	30	15	3.62144	−11.1776
9	100	30	20	3.82332	−11.6488
10	200	10	10	1.83949	−5.2939
11	200	10	15	2.20441	−6.8658
12	200	10	20	2.74452	−8.7693
13	200	20	10	1.87141	−5.4434
14	200	20	15	2.23044	−6.9678
15	200	20	20	2.76114	−8.8218
16	200	30	10	2.90291	−9.2567
17	200	30	15	2.25601	−7.0668
18	200	30	20	2.76138	−8.8225
19	300	10	10	1.47410	−3.3705
20	300	10	15	1.53834	−3.7411
21	300	10	20	1.66512	−4.4289
22	300	20	10	1.51067	−3.5834
23	300	20	15	1.57421	−3.9412
24	300	20	20	1.69943	−4.6061
25	300	30	10	1.54699	−3.7897
26	300	30	15	1.60980	−4.1354
27	300	30	20	1.73343	−4.7781

shows significant contribution on the specific wear rate and the factor red mud content ($p = 0.260$) and sliding velocity×red mud content ($p = 0.467$), present less significant contribution on specific wear rate.

CONFIRMATION EXPERIMENT

The confirmation experiment is the final test in the design of the experiment process. The purpose of the confirmation experiment is to validate the conclusions drawn during the analysis phase. It is performed by conducting a new set of factor settings $A_2B_3C_1$ to predict the specific wear rate. The estimated S/N ratio for specific wear rate can be calculated with the help of following predictive equation:

$$\hat{\eta}_1 = \bar{T} + (\bar{A}_2 - \bar{T}) + (\bar{B}_3 - \bar{T}) + [(\bar{A}_2\bar{B}_3 - \bar{T}) - (\bar{A}_2 - \bar{T}) - (\bar{B}_3 - \bar{T})] + \left(\bar{C}_1 - \bar{T}\right) + [(\bar{A}_2\bar{C}_1 - \bar{T}) - (\bar{A}_2 - \bar{T}) - (\bar{C}_1 - \bar{T})] + [(\bar{B}_3\bar{C}_1 - \bar{T}) - (\bar{B}_3 - \bar{T}) - (\bar{C}_1 - \bar{T})] \quad (4)$$

where $\hat{\eta}_1$ is the predicted average, $\bar{T}$ is the Overall experimental average, $\bar{A}_2$, $\bar{B}_3$, and $\bar{C}_1$ are the mean responses for factors and interactions at designated levels.

By combining like terms, the equation reduces to

$$\bar{\eta}_1 = \bar{A}_2\bar{B}_3 + \bar{A}_2\bar{C}_1 + \bar{B}_3\bar{C}_1 - \bar{A}_2 - \bar{B}_3 - \bar{C}_1 - \bar{T}. \quad (5)$$

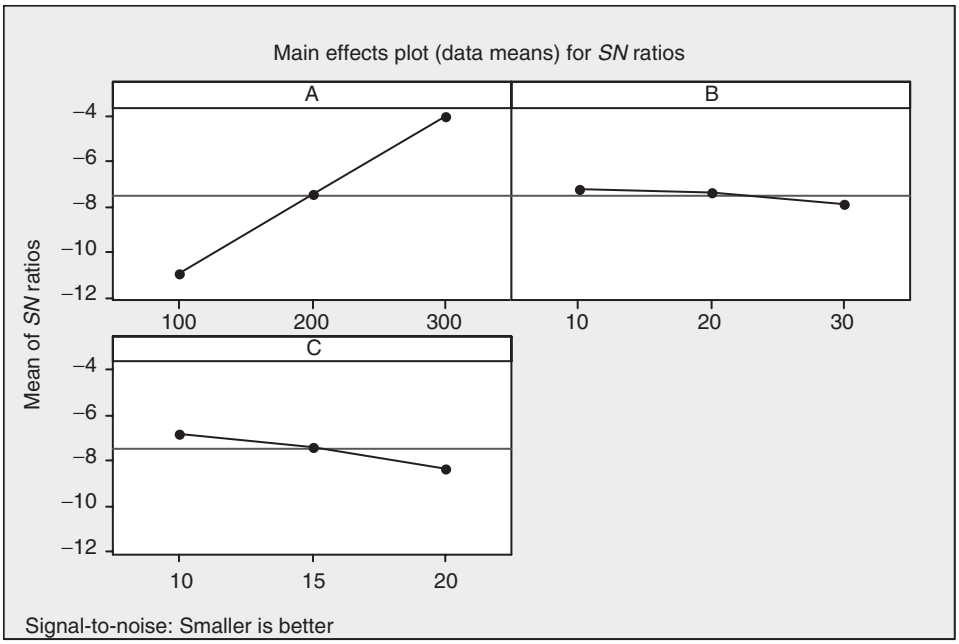

Figure 7. *Effect of control factors on specific wear rate.*

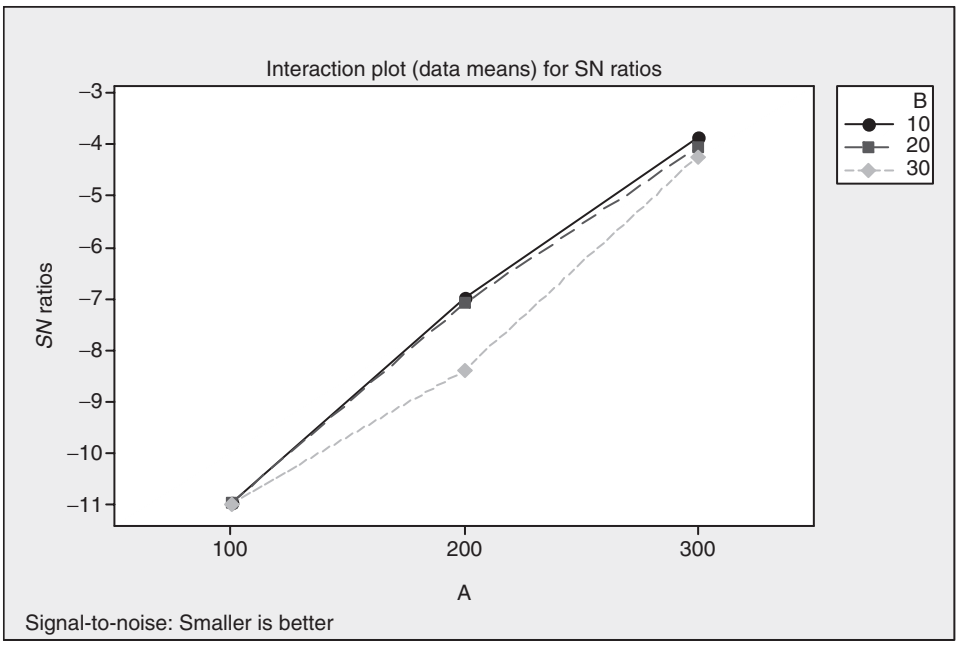

Figure 8. *Interaction graph between A × B for specific wear rate.*

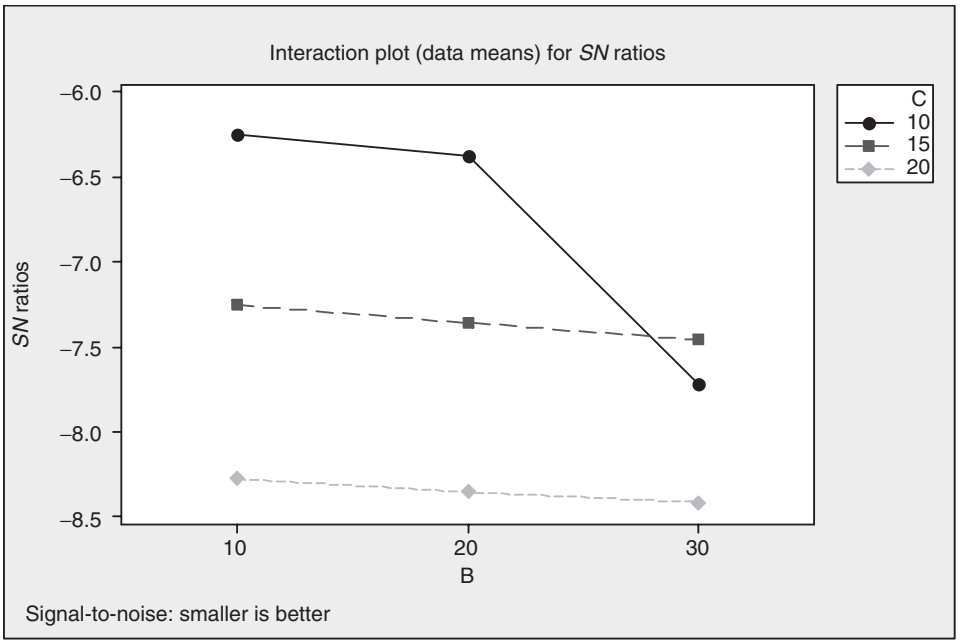

Figure 9. *Interaction graph between B × C for specific wear rate.*

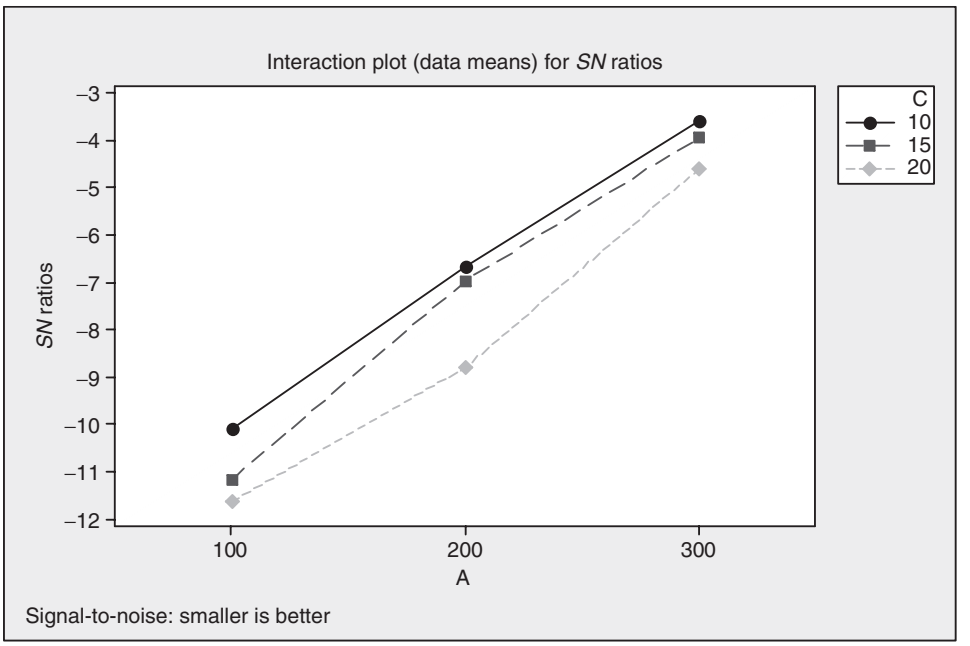

Figure 10. *Interaction graph between A × C for specific wear rate.*

Table 3. ANOVA table for specific wear rate.

Source	DF	SS	MS	F	P	Rank
A	2	17.2959	8.6479	224.98	0.000	1
B	2	0.12320	0.0616	1.60	0.260	3
C	2	0.94910	0.4745	12.35	0.004	2
$A \times B$	4	0.15170	0.0379	0.99	0.467	3
$A \times C$	4	0.29310	0.0733	1.91	0.203	1
$B \times C$	4	0.15880	0.0397	1.03	0.447	2
Error	8	0.30750	0.0384			
Total	26	19.2793				

Table 4. Results of the confirmation experiments for specific wear rate.

	Optimal control parameters	
	Prediction	Experimental
Level	$A_2\,B_3C_1$	$A_2\,B_3C_1$
S/N ratio for specific wear rate (dB)	−8.1399	−7.8948

A new combination of factor levels A_2, B_3, and C_1 is used to predict specific wear rate through prediction equation and it is found to be $\bar{\eta}_1 = -8.13991$ dB. For each performance measure, an experiment is conducted for a different factor combination and compared with the result obtained from the predictive equation as shown in Table 4.

The resulting model seems to be capable of predicting specific wear rate to a reasonable accuracy. An error of 3.01% for the S/N ratio of specific wear rate is observed. However, the error can be further reduced if the number of runs is increased. This validates the development of the mathematical model for predicting the measures of performance based on knowledge of the input parameters.

FACTOR SETTINGS FOR MINIMUM SPECIFIC WEAR RATE

In this study, an attempt is made to derive optimal settings of the control factors for minimization of specific wear rate. The single-objective optimization requires quantitative determination of the relationship between specific wear rate with combination of control factors. In order to express specific wear rate in terms of the mathematical model, the following equation is suggested:

$$Y = K_0 + K_1 \times A + K_2 \times B + K_3 \times C + K_4 \times A \times B + K_5 \times A \times C + K_6 \times B \times C. \quad (6)$$

Here, Y is the performance output terms and K_i ($i = 0, 1, \ldots, 6$) are the model constants. The constants are calculated using non-linear regression analysis with the help of SYSTAT 7 software and the following relations are obtained.

$$Y = 0.655 - 0.533A + 0.245B + 0.651C + 0.035A \times B - 0.341A \times C - 0.278B \times C$$
$$r^2 = 0.99. \quad (7)$$

The correctness of the calculated constants is confirmed as high correlation coefficient (r^2) to the tune of 0.99 is obtained for Equation (6) and therefore, the model is quite suitable to use for further analysis. Here, the resultant objective function to be maximized is given as:

$$\text{Maximize } Z = 1/f \tag{8}$$

where f is the normalized function for specific wear rate.

Subjected to constraints:

$$A_{\min} \leq A \leq A_{\max} \tag{9}$$

$$B_{\min} \leq B \leq B_{\max} \tag{10}$$

$$C_{\min} \leq C \leq C_{\max} \tag{11}$$

The min and max in Equations (9)–(11) show the lowest and highest control factor settings (control factors) used in this study (Table 1).

The genetic algorithm (GA) is used to obtain the optimum value for single-objective outputs to optimize the single-objective function. The computational algorithm is implemented in Turbo C^{++} and run on an IBM Pentium IV machine. Genetic algorithms (GAs) are mathematical optimization techniques that simulate a natural evolution process. They are based on Darwinian theory, in which the fittest species survives and propagate while the less successful tend to disappear. The genetic algorithm mainly depends on three types of operators, viz., reproduction, crossover, and mutation. Reproduction is accomplished by copying the best individuals from one generation to the next, which is often called an elitist strategy. The best solution is monotonically improving from one generation to the next. The selected parents are submitted to the crossover operator to produce one or two children. The crossover is carried out with an assigned probability, which is generally rather high. If a number randomly sampled is inferior to the probability, the crossover is performed. The genetic mutation introduces diversity in the population by an occasional random replacement of the individuals. The mutation is performed based on an assigned probability. A random number is used to determine if a new individual can be produced to substitute the one generated by crossover. The mutation procedure consists of replacing one of the decision variable values of an individual while keeping the remaining variables unchanged. The replaced variable is randomly chosen and its new value is calculated by randomly sampling within its specific range. In genetic optimization, population size, probability of crossover, and mutation are set at 50, 75, and 5%, respectively, for all the cases. The number of generations is varied until the output is converted. Table 5 shows the optimum conditions of the control factors with optimum performance output which gives a better combination of a set of input control factors. The pattern of convergence of performance output with number of generations is shown in Figure 11.

CONCLUSIONS

This experimental investigation into the sliding wear behavior of red mud filled polyester matrix composites leads to the following conclusions.

1. Red mud, an industrial waste, can be used as a potential filler material in polyester matrix composites. It has marginal effects on the mechanical properties such as

Table 5. Optimum conditions for performance output.

Control factors and performance characteristics	Optimum conditions
A: Sliding velocity (cm/s)	107.40
B: Redmud content (%)	29.43
C: Normal load (N)	19.82
Specific wear rate (mm^3/N-m)	3.7114

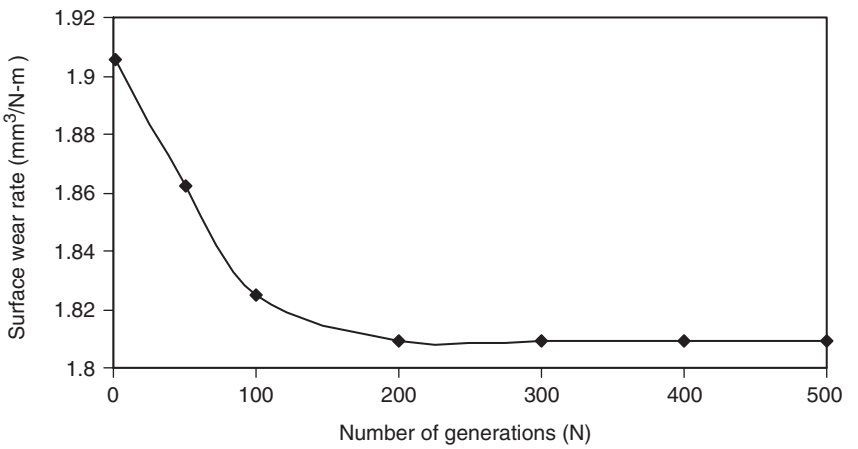

Figure 11. *Convergence curve.*

hardness and tensile strength of the composites. The compatibility of red mud particles with polyester resin is fairly good.

2. Dry sliding wear characteristics of these composites can be successfully analyzed using Taguchi experimental design scheme. The Taguchi method provides a simple, systematic, and efficient methodology for the optimization of the control factors.
3. Factors like sliding velocity, normal load, and filler content (wt% of red mud) in order of priority are significant to minimize the specific wear rate. Although the effect of filler content is less compared to other factors, it cannot be ignored because it shows significant interaction with other factors like the normal load.
4. Red mud is found to possess good filler characteristics as it improves the sliding wear resistance of the composite. Scanning electron microscopy suggests that particle detachment due to the tearing of the thermoplastic matrix body by the sharp edges of the filler particles is the dominant wear mechanism occurring during the contact of composite with the counter body. It leads to the conclusion that spherodized red mud particles may be preferred for filling purposes during composite making.
5. The rationale behind the use of the genetic algorithm lies in the fact that it has the capability of finding the global optimal parameter settings whereas the traditional optimization techniques are normally stuck at the local optimum values. The optimum settings are found to be a sliding velocity of 107.40 cm/s, red mud content of 29.43 wt%,

a normal load of 19.82 N, and the resulting specific wear rate of 3.7114 mm^3/N-m as far as the present experimental conditions are concerned.

6. In future, this study can be extended to polymer matrix composites using other filler materials.

REFERENCES

1. Katz, H. S. and Mileski, J. V. (1987). *Handbook of Fillers for Plastics*, November 30, A Von Nostrand Reinhold Book.
2. Mareri, P., Bastide, S., Binda, N. and Crespy, A. (1998). Mechanical Behaviour of Polypropylene Composites Containing Fine Mineral Filler: Effect of Filler Surface Treatment, *Composites Science and Technology*, **58**(6): 747–752.
3. Järvelä, P. A. and Järvelä, P. K. (1996). Multi-Component Compounding of Polypropylene, *Journal of Materials Science*, **31**(14): 3853–3859.
4. Rusu, M., Sofian, N. and Rusu, D. (2001). Mechanical and Thermal Properties of Zinc Powder Filled High Density Polyethylene Composites, *Polymer Testing*, **20**(44): 409–417.
5. Barta, S., Bielek, J. and Dieska, P. (1997). Study of Thermophysical and Mechanical Properties of Particulate Composite Polyethylene–$CaCO_3$, *Journal of Applied Polymer Science*, **64**(8): 1525–1530.
6. Jang, B. Z. (1994). Advanced Polymer Composites: Principles and Applications. ASM International.
7. Gregory, S. W., Freudenberg, K. D., Bhimaraj, P. and Schadler, L. S. (2003). A Study on the Friction and Wear Behavior of PTFE Filled with Alumina Nanoparticles, *Wear*, **254**: 573–580.
8. Jung-il, K., Kang, P. H. and Nho, Y. C. (2004). Positive Temperature Coefficient Behavior of Polymer Composites Having a High Melting Temperature, *J. Appl. Polym. Sci.*, **92**: 394–401.
9. Nikkeshi, S., Kudo, M. and Masuko, T. (1998). Dynamic Viscoelastic Properties and Thermal Properties of Powder-epoxy Resin Composites, J. *Appl. Polym. Sci.*, **69**: 2593–2598.
10. Zhu, K. and Schmauder, S. (2003). Prediction of the Failure Properties of Short Fiber Reinforced Composites with Metal and Polymer Matrix, *Comput. Mater. Sci.*, **28**: 743–748.
11. Tavman, I. H. (1997). Thermal and Mechanical Properties of Copper Powder fiLled Poly(ethylene) Composites, *Powder Technol.*, **91**: 63–67.
12. Mahapatra, B. K., Rao, M. B. S., Bhima Rao, R. and Paul, A. K. (2000). Characteristics of Red Mud Generated at NALCO Refinery, Damanjodi, India, *Light Metals*, 161–165.
13. Solimar, K., Sajo, I., Steiner, J. and Zoldi, J. (1992). Characteristics and Separability of Red Mud, *Light Metals*, 209–223.
14. Sahin, S. (1998). Correlation Between Silicon-dioxide and Iron-oxide Contents of Red Mud Samples, *Hydrometallurgy*, **47**: 371–376.
15. Wang, Q., Gu, S., Han, Z. and Li, D. (1998). Irreversible Thixotropic Behaviour of Red Mud Slurry and Exploitation in Dry Disposal Process, *Nonferrous Metals* (*China*), **50**(2): 85–91.
16. Wong, K. W.-Y. and Truss, R. W. (1994). Effect of Flyash Content and Coupling Agent on the Mechanical Properties of Flyash-filled Polypropylene, *Composites Science and Technology*, **52**(3): 361–368.
17. Srivastava, V. K. and Shembekar, P. S. (1991). Mechanical Properties of E-glass Fibre Reinforced Nylon 6/6 Resin Composites, *Journal of Materials Science*, **26**: 6693–6698.
18. Durand, J. M., Vardavoulias, M. and Jeandin, M. (1995). Role of Reinforcing Ceramic Particles in the Wear Behaviour of Polymer-based Model Composites, *Wear*, **183**: 833–839.
19. Mahapatra, S. S. and Patnaik, A. (2006). Optimization of Wire Electrical Discharge Machining (WEDM) Process Parameters using Genetic Algorithm, *Int. J. Adv. Manuf. Technol.*, DOI.10.1007/s00170-006-0672-6.
20. Mahapatra, S. S. and Patnaik, A. (2006). Parametric Analysis and Optimization of Drilling of Metal Matrix Composites based on the Taguchi Method, *The International Journal for Manufacturing Science and Technology*, **8**(1): 5–12.
21. Patnaik, A., Satapathy, A., Mahapatra, S. S. and Dash, R. R. (2007). A Modeling Approach for Prediction of Erosion Behavior of Glass Fiber–Polyester Composites, *J Polym Res.*, DOI 10.1007/s10965-007-9154-2.
22. Glen, S. P. (1993). *Taguchi Methods: A Hands on Approach*, Addison-Wesley, New York.